JOURNAL OF GEOPHYSICAL RESEARCH, VOL. 108, NO. C5, 8084, doi:10.1029/2001JC001147, 2003

Transport and variability of the Antarctic Circumpolar Current in Drake Passage

S. A. Cunningham, S. G. Alderson, and B. A. King
Southampton Oceanography Centre, Southampton, UK

M. A. Brandon[1]
British Antarctic Survey, High Cross, Cambridge, UK

Received 14 September 2001; revised 9 September 2002; accepted 31 March 2003; published 31 May 2003.

[1] The baroclinic transport of the Antarctic Circumpolar Current (ACC) above 3000 m through Drake Passage is 107.3 ± 10.4 Sv and has been steady between 1975 and 2000. For six hydrographic sections (1993–2000) along the World Ocean Circulation Experiment (WOCE) line SR1b, the baroclinic transport relative to the deepest common level is 136.7 ± 7.8 Sv. The ACC transport is carried in two jets, the Subantarctic Front 53 ± 10 Sv and the Polar Front (PF) 57.5 ± 5.7 Sv. Southward of the ACC the Southern Antarctic Circumpolar Current transports 9.3 ± 2.4 Sv. We observe the PF at two latitudes separated by 90 km. This bimodal distribution is related to changes in the circulation and properties of Antarctic Bottom Water. Three realizations of the instantaneous velocity field were obtained with lowered ADCPs. From these observations we obtain near-bottom reference velocities for transport calculations. Net transport due to these reference velocities ranges from −28 to 43 Sv, consistent with previous estimates of variability. The transport in density layers shows systematic variations due to seasonal heating in near-surface layers. Volume transport-weighted mean temperatures vary by 0.40°C from spring to summer; a seasonal variation in heat flux of about 0.22 PW. Finally, we review a series of papers from the International Southern Ocean Studies Program. The average yearlong absolute transport is 134 Sv, and the standard deviation of the average is 11.2 Sv; the error of the average transport is 15 to 27 Sv. We emphasize that baroclinic variability is an important contribution to net variability in the ACC. *INDEX TERMS:* 4594 Oceanography: Physical: Instruments and techniques; 4512 Oceanography: Physical: Currents; 4532 Oceanography: Physical: General circulation; 4536 Oceanography: Physical: Hydrography; *KEYWORDS:* Drake Passage, Antarctic Circumpolar Current, hydrography, acoustic Doppler current profiler, transport, ISOS

Citation: Cunningham, S. A., S. G. Alderson, B. A. King, and M. A. Brandon, Transport and variability of the Antarctic Circumpolar Current in Drake Passage, *J. Geophys. Res.*, *108*(C5), 8084, doi:10.1029/2001JC001147, 2003.

1. Introduction

[2] The Southern Ocean is a major component of the coupled ocean-atmosphere climate system. It connects all the other major oceans and influences the water mass characteristics of the deep water over a large portion of the world. It is an area of net heat loss from the ocean to the atmosphere, and is the conduit for substantial heat and freshwater exchange between the ocean basins. The World Ocean Circulation Experiment specified a number of regions in the global ocean where repeat observations were important to gauge the representativeness of single section realisations of properties and transport: a section across the Antarctic Circumpolar Current in Drake Passage was identified as one such section. Estimates of a mean global ocean circulation are now limited by the uncertainty introduced by oceanic variability [*Ganachaud and Wunsch*, 2000]. Improving the accuracy of such estimates requires data sets that represent the true temporal average of properties and the circulation. In this paper we report the transport and variability observed from six hydrographic sections from 1993 to 2000. While we are sanguine as regards the contribution that six sections make to determining the true temporal average of the Antarctic Circumpolar Current transport, consideration of these sections and comparison to historical data does suggest what observations would be necessary to determine such an average.

[3] The canonical value of net transport through Drake Passage is 134 ± 11.2 Sv (± standard deviation of the annual average) [*Whitworth and Peterson*, 1985]. Whitworth and co-authors determined this transport estimate from a yearlong current meter array, pressure gauges and hydrographic data. The data and the analysis methods that lead to this transport estimate are quite detailed and are developed across the three papers by *Whitworth et al.* [1982], *Whit-*

[1]Now at The Open University, Milton Keynes, UK.

0148-0227/03/2001JC001147

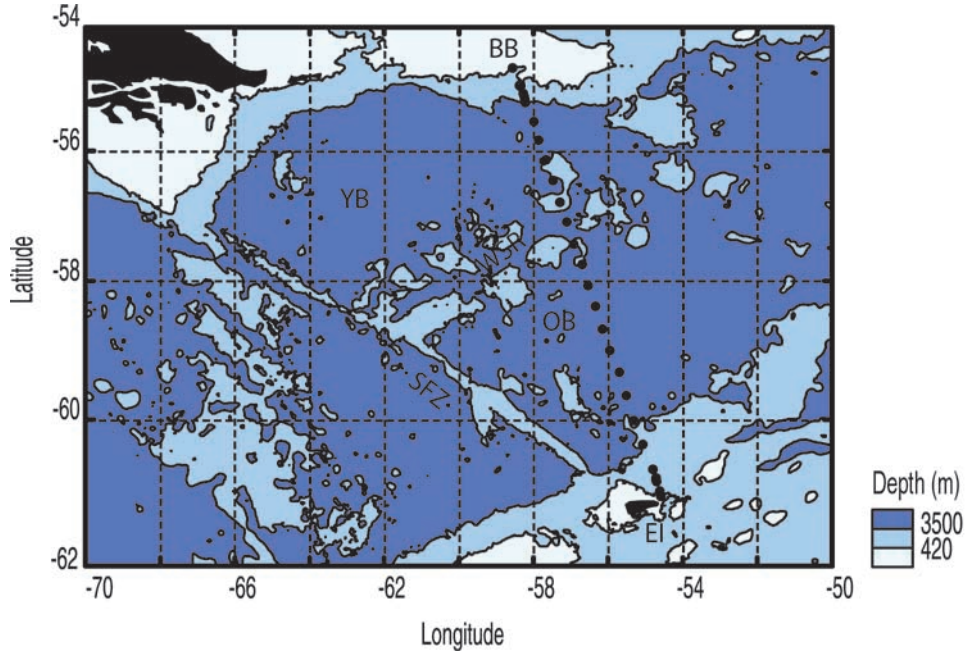

Figure 1. Bathymetry of the Drake Passage from *Sandwell and Smith* [1997]. Flow deeper than 3500 m is blocked by the Shackleton Fracture Zone [*Thompson*, 1995], and flow shallower than about 400 m can pass over the sill between Burdwood Bank and South America. The SR1b CTD section is indicated by the black dots. Bathymetric features are: Burdwood Bank (BB), Yagan Basin (YB), Ona Basin (OB), Elephant Island (EI), Shackleton Fracture Zone (SFZ), and West Scotia Ridge (WSR).

worth [1983], *Whitworth and Peterson* [1985]. Reviewing these papers, we draw together the critical steps for converting the raw data to transport estimates. This makes clear that the uncertainty of the average transport lies between 11 and 20% of the average: the average transport of the Antarctic Circumpolar Current is less well known than is often supposed. The variability in transport is commonly assumed to stem from variability in the barotropic component of the flow. *Whitworth and Peterson* [1985] used across passage pressure difference correlated to net transport to derive a function to predict transport from across passage pressure difference. They argued that this gave an accurate representation of variability in net transport. However, it is clearly seen in their results that across passage pressure differences do not account for variability in the net transport due to changes in the baroclinic field. Reinterpreting their analysis and in comparison with the recent sections presented here we argue for a different interpretation of the net variability: that barotropic and baroclinic variations contribute in roughly equal portions to the net variability and that a monitoring system to measure the average transport and variability need to determine the variability in both barotropic and baroclinic components of the flow.

[4] This paper is divided into the following sections: section 2, describing the hydrographic observations made on WOCE section SR1b between 1993 and 2000; section 3, a 25 year baroclinic transport time series through Drake Passage from 1975 to 2000; section 4, a detailed description of the variability in baroclinic transport seen on the WOCE sections; section 5, estimates of the geostrophic transport in neutral density layers, total net transport calculated using lowered acoustic Doppler current profiler data to provide a near-bottom reference velocity for the geostrophic velocity and the zonal temperature flux; section 6, a review of the ISOS transport and variability estimates; section 7, the relative importance of barotropic versus baroclinic variability; and section 8, summary and conclusions.

2. Data

[5] Since 1993 the Southampton Oceanography Centre and British Antarctic Survey (BAS) have occupied the WOCE section SR1b six times. This hydrographic work was done from the UK's icebreaker the RRS *James Clark Ross* enroute from the Falkland Islands to BAS bases on the Antarctic Peninsula. Four of the sections were occupied in November at the beginning of Austral Spring and two in late December/January and February. Some seasonal stratification is evident from the sections late in the season.

[6] As a minimum the section consists of 31 full depth CTD stations (Figure 1) and shipboard ADCP providing velocity profiles in the upper 200 m. In some years additional observations have enhanced the basic hydrography (see Table 1). In particular lowered ADCP data were collected at each CTD station in 1996, 1997 and November 2000. CTD data quality are generally excellent, particularly temperature and pressure which meet the requirements for WOCE repeat section hydrography [*WHPO*, 1991]. Salinities meet WOCE repeat hydrography standards but have been less consistently good overall [*Bacon et al.*, 2000]. CTD salinities have been calibrated against up to 12 vertical salinity samples at each station, these samples being analyzed on a Guildline Autosal against IAPSO standard seawaters.

[7] A 150 kHz broadband self contained RD Instruments ADCP was mounted on the CTD frame. Two instruments have been used; nearly all data are from an instrument with a

Table 1. Baroclinic Transport (Positive Eastward) Above and Relative to Zero at dbar T_{3000}[a]

Date	T_{3000}, Sv	Notes
27 Feb. to 7 March 1975	111	Melville section II
16–22 March1975	106	Melville section V
26 Feb. to 3 March 1976	110	Thomson
19–24 Jan. 1977	75	Melville
20–27 Jan. 1979	110	Melville
15–20 April 1979	102	Yelcho
8 Jan. to 13 Feb. 1980	105	Atlantis II
23–29 Jan. 1990	107	SR1: Roether
21–26 Nov. 1993	110	SR1b
15–21 Nov. 1994	115	SR1b
15–20 Nov. 1996	105	SR1b, LADCP
29 Dec. to 7 Jan. 1997	118	SR1b, LADCP, nutrients, and O_2 data
11–16 Feb. 2000	118	SR1b
23–28 Nov. 2000	110	SR1b, LADCP
Mean	107.3	
SD	10.4	

[a]The transport for sections from 1975 and 1980 were reported by *Whitworth and Peterson* [1985] and were occupied at the western end of Drake Passage from Cape Horn to Livingston Island. The 1990 section by *Roether et al.* [1993] was on WOCE section A21 at the western end of Drake Passage. WOCE southern repeat section 1b (SR1b) runs from Burdwood Bank at the northern edge of Drake Passage to Elephant Island at the southern edge (Figure 1). The February 2000 cruise is in season 1999/2000 and is referred to as 1999 throughout. Statistics are as follows: T_{3000}, 1975–1980, μ = 102.7 Sv, σ = 12.6; 1975–1980, excluding 1977, μ = 107.3 Sv, σ = 3.6; 1990–2000, μ = 111.9 Sv, σ = 5.2, where μ is the mean and σ is standard deviation.

20° transducer head; a few stations have been taken with a 30° instrument. The instrument configuration has been 16 times 10 m bins; we use a 2 s ensemble, consisting of one bottom-track (BT) and one water-track (WT) ping. If the bottom is not found, the instrument waits 50 s before emitting another BT ping. Water track data were processed within the framework of the software suite developed at the University of Hawaii and made available by Dr Eric Firing and coworkers, though these analyses have not been used in this paper. See *Visbeck* [2002] for a description of data methodology and an alternative inverse solution method. Bottom-track data were typically collected within 250 to 300 m off the bottom. They were processed from ASCII files exported from the PC used to configure the ADCP.

[8] Near bottom, the LADCP measures the speed of the package over the ground with dedicated BT pings. Each 2-s ensemble consists of a BT ping followed by a WT ping. BT pings are used to determine height off bottom and absolute velocity of package; WT pings determine velocity of water relative to package, as usual. Absolute velocity of water over the ground is then a simple vector addition of the BT and WT velocities. Typically, near-bottom velocities can be determined between 50 and 250 m off bottom, in water depths greater than 3000 m.

[9] The absolute near-bottom velocity error can be estimated. For a 150 kHz ADCP over a profile range of around 160 m with 16 m bins the standard deviation of each water track and bottom track velocity measurement is about 1 cms^{-1} [*RD Instruments*, 1995, Appendix F]. If we assume that the absolute velocity error has a contribution from the bottom track and from the water track, and there are about 50 independent estimates of velocity in each 5 m bin then the error of the near-bottom velocities is approximately $\sqrt{2}/\sqrt{50} = 0.2$ cm/s and is an order of magnitude better than the stochastic error in a typical top to bottom profile derived from water track shear estimates. Water-track shear estimates are discussed by *King et al.* [2001].

[10] A single near-bottom reference velocity is calculated from the absolute near-bottom data as follows. For each ensemble, the BT and WT pings are combined to provide discrete absolute water velocities, corresponding to the instrument bins. The complete set of such absolute bin velocities are gridded into a vertical profile, with a 5-m gridsize in the vertical. The gridded cells in this vertical profile are then reduced to a mean "near-bottom velocity," and a standard deviation which combines both the instrumental error and any shear present in the bottom few hundred meters of the water column. Recognising that instrumental errors may be greatest at either maximum range off bottom, or near the bottom, a new mean is calculated by excluding those cells more than twice the standard deviation from the original mean. Next, using the Topex/Poseidon tidal model of *Egbert and Bennett* [1994] we remove the average barotropic tide over the period of the bottom track profile. The tidal velocities predicted by this model never contribute more than ±2 Sv to the net section transport for the different occupations of the section. Thirdly, pairs of the near-bottom reference velocities are averaged to determine reference velocities at the positions of the geostrophic profiles. These reference velocities are added to the geostrophic profiles calculated relative to deepest common level. *Beal and Bryden* [1999] use a similar method in the Agulhas Current, adding the water track velocities to geostrophic shear to derive net geostrophic velocities.

3. 25 Year Baroclinic Transport Time Series

[11] A 25 year time series of baroclinic transports through Drake Passage can be assembled from hydrographic sections at the western and eastern ends of Drake Passage. The western sections date from 1975 to 1990 and the eastern sections (WOCE SR1b) from 1993 to 2000 so that there are no overlaps in time or space. The zonal separation of the two sections introduces two sources of uncertainty. The first is that below 3500 m flow through Drake Passage is blocked by the Shackleton Fracture Zone (Figure 1). To combine the western and eastern sections we consider transport relative to and above 3000 dbar, ignoring any possible additions to the flow between the sections at the surface or from below 3000 dbar. Second, between the western and eastern sections there is sill of depth 420 m between Burdwood Bank and South America, so that there is the potential for upper ocean flow-passing through western Drake Passage to be lost to the South Atlantic without crossing the eastern Drake Passage section. We do not have the data to assess whether these problems are significant, but they contribute to uncertainty in the transport time series assembled below.

[12] The time series of baroclinic transport (Table 1) demonstrates the long-term stability of the baroclinic transport. From 1975 to 1980 the mean transport is 102.7 ± 12.6 Sv and from 1990 to 2000 the mean transport is 112.2 ± 5.6 Sv. A student-t test with 95% confidence limits suggests that there is no difference in the means of these two groups.

[13] The 1977 transport of 75 Sv seems anomalously low. However, the short-term variability in baroclinic transport is large [*Whitworth*, 1983, Figure 7]. From moorings on either

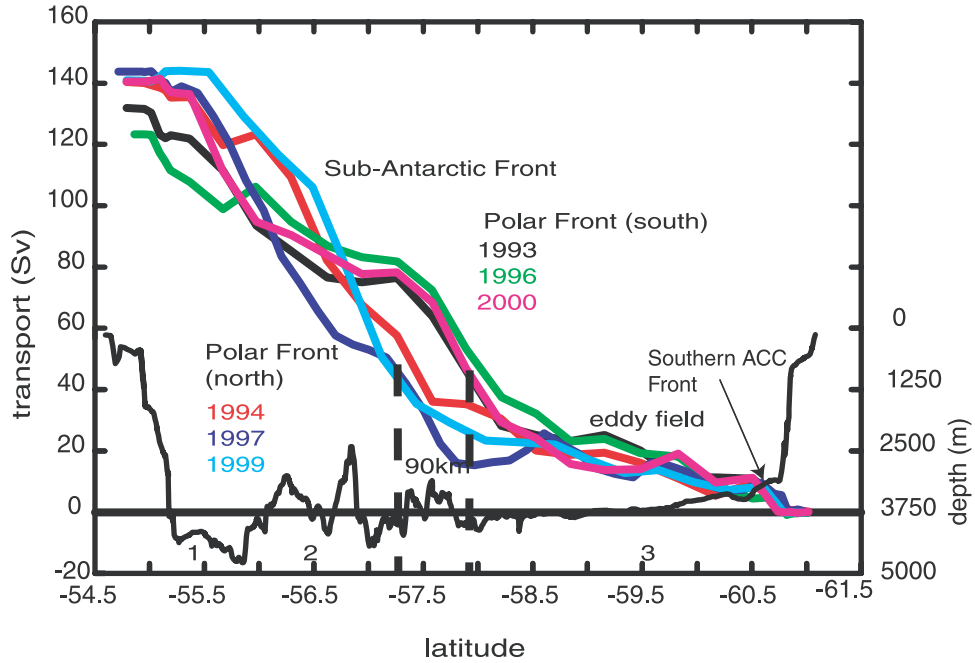

Figure 2. Section-integrated (south to north) baroclinic transport relative to the deepest common level (DCL) for the six hydrographic sections along SR1b between 1993 and 2000: the average transport is 136.7 ± 7.8 Sv. The locations and names of fronts (following *Orsi et al.* [1995]) are shown. Bathymetry from the ship's echosounder is also shown by the scale on the right-hand side. The position of the Polar Front is given a position either north or south based on where the section-integrated transport rises through 50 Sv.

side of Drake Passage that measured dynamic height *Whitworth* [1983] calculated a yearlong time series of the baroclinic transport. Relative to and above 2500 m (January 1979 to February 1980) the mean transport was 87 ± 5.5 Sv with a range of 30 Sv (minimum 70 to a maximum 100 Sv). Transport variations greater than 15 Sv occur over periods of two weeks and there are at least ten cycles through the year with peak to trough variations in transport of at least 10 Sv. The absolute transport above 2500 m for the period January 1979 to February 1980 is 124.7 ± 9.9 Sv with minimum and maximum values of 95 and 149 Sv, a range of 56 Sv [*Whitworth and Peterson*, 1985, Figure 3b] The baroclinic transport estimate in 1977 of 75 Sv probably represents a short period variation and the yearlong time series of baroclinic transport has transport values as low as this and the range of total transport could comfortably accommodate a drop in the baroclinic transport of 31 Sv.

[14] We conclude that over 25 years from 1975 to 2000, the baroclinic transport through Drake Passage has no discernible trend. The 25 year mean baroclinic transport relative to and above 3000 dbar is 107.3 ± 10.4 Sv with minimum and maximum transports of 75 and 118 Sv respectively, a range of 43 Sv.

4. Baroclinic Transport Relative to the Deepest Common Level (WOCE Section SR1b 1993 to 2000)

[15] Between 1975 and 2000 above 3000 m the baroclinic transport does not have any long-term trend, though, it is evident that there is year to year variability in the section-integrated transport. In this section we will examine in detail the net baroclinic transport relative to the deepest common level (DCL) through the WOCE SR1b section for six hydrographic sections between 1993 and 2000. The section-integrated baroclinic transport (Figure 2 and Table 2) is 136.7 ± 7.8 Sv relative to zero at the DCL: a few Sv more than the net transport measured by the ISOS array [*Whitworth and Peterson*, 1985] of 133.8 ± 11.2 Sv.

[16] The transport occurs at three fronts in Drake Passage (Figure 2). From south to north these are (following the nomenclature of [*Orsi et al.*, 1995] the Southern ACC front around 60.75°S, the Polar Front nominally around 57.5°S, and the Subantarctic Front nominally around 56°S. The Polar Front and Subantarctic Front together constitute the ACC and span 3° of latitude, filling half the width of Drake Passage.

[17] The Southern ACC front is located at the continental shelf break and delineates the boundary between warm Deep Water and well mixed cold (and fresh) continental

Table 2. Baroclinic Transport (Positive Eastward) Relative to Zero at the DCL for the Six SR1b Hydrographic Sections

Year	Transport, Sv	Polar Front Position
1993	131.4	South
1994	140.4	North
1996	123.1	South
1997	143.8	North
1999	140.9	North
2000	140.4	South
Mean	136.7	
SD	7.8	

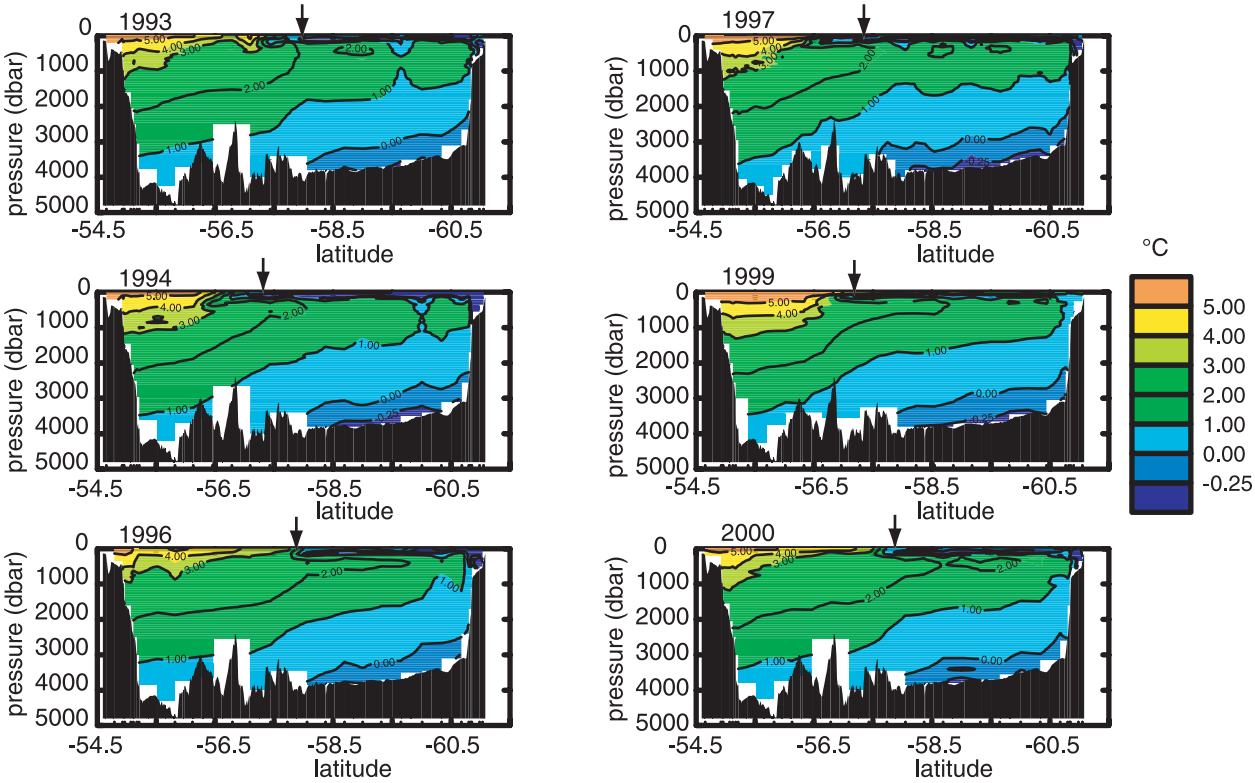

Figure 3. (a) Potential temperature section for the six SR1b occupations. Bathymetry from the ship's echosounder is colored black. (b) Same as in Figure 3a but for geostrophic velocity relative to zero at the Deepest Common Level (DCL). Arrows indicate the southern boundary of the Polar Front identified from a θ/S transition as described in the text.

water masses sitting on the continental shelf. A narrow jet is supported by this water mass boundary and transports 9.3 ± 2.4 Sv.

[18] The section-integrated transport of the Polar Front has a bimodal distribution in latitudinal position. In 1993, 1996 and 2000 (southerly years) the Polar Front is found at 57.9°S and in 1994, 1997 and 1999 (northerly years) is found 90 km further north at 57.2°S (Figure 2) (taken to be where the section-integrated transport reaches 50 Sv). The Polar Front is always found south of the valley in the centre of the West Scotia Ridge. Possible reasons for the bimodal distribution are examined later.

[19] It is convenient to identify the location of the Polar Front using a value of the transport in Figure 2. However, the equivalent result of northern and southern years could have been inferred from a study of water mass properties. The θ/S curves for this section always show a striking change approaching the Polar Front from the south. Northward of the Polar Front the adjustment of properties is more continuous, and occurs at different depths for different station pairs, so that from the southern side of the Polar Front to the northern side of the Subantarctic Front should be considered as a transition zone. If all six sections are plotted on a θ/S diagram, there is an obvious gap that, conveniently, includes the values θ = 1.0°C, S = 34.20. The location of the Polar Front can be identified by finding the station pair at which the θ/S curve jumps across this point; these locations are shown as arrows in Figures 3a and 3b.

[20] North of the Polar Front the Subantarctic Front is confined to the Yagan Basin between Burdwood Bank and the West Scotia Ridge. When the Polar Front is in its southerly position there is a plateau in the section-integrated transport between the two fronts (Figure 2), and the Subantarctic Front maximum surface velocity is located in the central Yagan Basin. In 1993 and 1996 a narrow jet transporting around 10 Sv (Figure 3a) is found north of the Subantarctic Front pressed tightly against Burdwood Bank.

[21] When the Polar Front is in its northerly position in 1994 and 1999 the integrated transport across the Polar Front and Subantarctic Front (Figure 2) is continuous so that the fronts appear merged. This is particularly clear in 1999 (Figure 3b) when the Polar Front and Subantarctic Front have merged to form a jet with much higher surface velocities than in any other year. It seems that when the Polar Front is in its more northerly position it can interact with the Subantarctic Front and move northward onto the West Scotia Ridge. In 1997 the Polar Front and Subantarctic Front are separated by a plateau of slowly increasing northward transport: there is clear separation of the surface jets and the Subantarctic Front has split into three separate jets.

[22] For the Polar Front in its southerly position and clearly separated from the Subantarctic Front the transport carried by these fronts is 57.5 ± 5.7 Sv and 53 ± 10 Sv respectively. With the Polar Front and Subantarctic Front merged their transports combine to around 110 Sv.

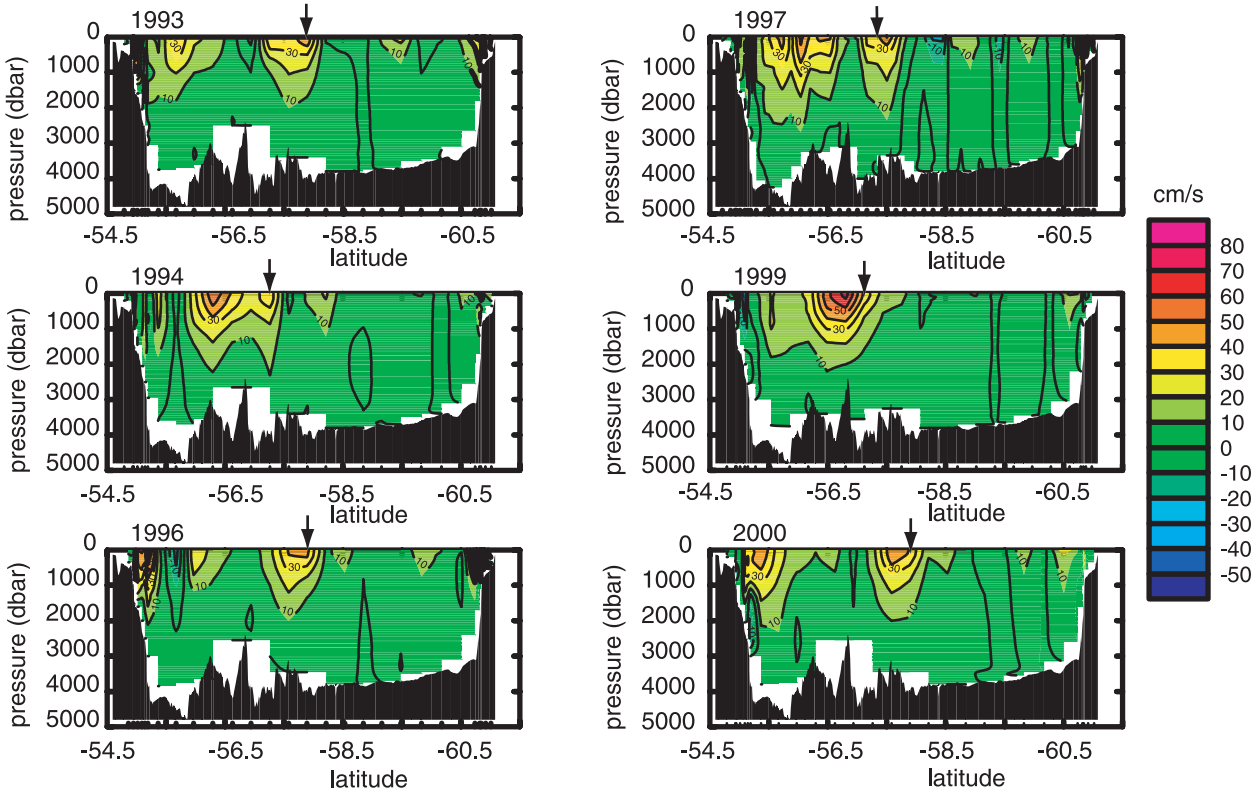

Figure 3. (continued)

[23] There is a correspondence, though not exact, between the position of the Polar Front and the net transport. The two smallest values of net baroclinic transport occur when the Polar Front is south (1993 and 1996) and three for the four largest values of net transport occur when the Polar Front is in its northerly position (1994, 1997 and 1999). The remaining year 2000 does not fit the pattern. Quantitatively, when the Polar Front is south (93, 96, 00) the net transport is 131.9 ± 8.6 Sv and when the Polar Front is north (94, 97, 99) the net transport is 141.7 ± 1.8 Sv.

[24] Finally we discuss the net transport through the section between the Southern ACC and Polar fonts. This region has weak vertical stratification, seems to be free of persistent jets and is populated with deeply penetrating eddies: typically one to three were present during our occupations of this section. These eddies have weak vertical velocity shear and the surface velocities are typically $10-15$ cms^{-1} (Figures 3a and 3b). The recirculating baroclinic transport associated with these eddies is of the order 10 Sv (Figure 2). We will see later that these eddies have large bottom velocities that increase the recirculating transport to values as large as ±25 Sv. The Circumpolar Deep Water rises most rapidly across the Polar Front but continues to rise to the south through this eddy field. The net transport between the Southern ACC and Polar fonts is around 16 Sv.

4.1. Variability of the Polar and Subantarctic Fronts

[25] In the previous section we noted a bimodal distribution of the section-integrated transport associated with the latitudinal position of the Polar Front and a correspondence between this position and the net baroclinic transport relative to the DCL. From our observations we note the following that may be related to the Polar Front position: (1) When the Polar Front is to the north, Antarctic Bottom Water colder than −0.3°C is found in a thin layer at the bottom across the whole Ona Basin (Figure 3a). Conversely, when the Polar Front is in a southerly position the Antarctic Bottom Water temperatures across the Ona Basin are significantly warmer. Temperature anomalies have a maximum peak to trough amplitude of 0.14°C. (2) The Polar Front position is topographically controlled. We now examine each of these in more detail.

4.2. Antarctic Bottom Water

[26] The variability of Antarctic Bottom Water in the Ona Basin has been examined by *Rubython et al.* [2001] using a four yearlong time series of bottom temperatures at 59°43.7S, 55°29.5W from a bottom pressure recorder (located on the SR1b line) in a depth of 3690 m.

[27] The source of Antarctic Bottom Water in the Ona Basin is Weddell Sea Deep Water; a variety of air-sea-ice interactions round the margins of the Weddell Sea form Weddell Sea Deep Water and Weddell Sea Bottom Water. 1.5 Sv of cold dense Weddell Sea Deep Water flows through the Orkney Passage [*Locarnini et al.*, 1993] where the sill depth is around 3500 m (the Orkney Passage is located on the South Scotia Ridge at 46.5°W). Within the Scotia Sea the Weddell Sea Deep Water changes names to become Antarctic Bottom Water and travels westward as a deep western boundary current into the Ona Basin until further westward progress is restricted by the Shackleton Fracture Zone. The observed temperature variability in the Antarctic Bottom Water in the Ona Basin was related by

Rubython et al. [2001] to changes in the composition of the Weddell Sea Deep Water in the Weddell Sea that were advected to the Ona Basin. Changes in the deep circulation patterns and in the origins of Antarctic Bottom Water were considered as causes of the observed variability in the Ona Basin and some qualitative arguments were advanced to reject these ideas, and to support the idea that Antarctic Bottom Water variability was due to variability in the properties of Weddell Sea Deep Water in the Weddell Sea. However, a paucity of data means that the circulation rates, pathways and mixing of Antarctic Bottom Water between Orkney Passage and the Ona Basin are not well known.

[28] Sir George Deacon [*Deacon*, 1937, p. 21] first suggested that the Polar Front position (where the warm Deep Water rises sharply to the south) is controlled by the circulation of the bottom water.

> A consideration of the circumstances shows that the warm Deep Water climbs toward the surface because it can only continue its southward movement above the Antarctic Bottom Water. The locality and steepness of the upward movement must therefore be determined by factors which govern the flow of bottom water. This conclusion is justified by observations which show that wherever the northward flow of the bottom water is influenced by the configuration of the seafloor the movements of the deep water are altered conformably. Since the latitude in which the deep water makes its sudden upward movement is determined by factors which govern the flow of bottom water, it follows that the same factors fix the position of the Antarctic Convergence.

As a corollary, variability in the bottom water circulation ought to be mirrored in the position of the Polar Front.

[29] *Rubython et al.* [2001] investigated the relationship between the surface position of the Polar Front and Antarctic Bottom Water temperature anomalies in the Ona Basin. Using the Along-Track Scanning Radiometer of ERS1 to determine sea surface temperature, they constructed a time series of Polar Front position (the position of the Polar Front was taken to be the position of the maximum SST gradient). Because this time series did not look like the Antarctic Bottom Water temperature anomaly time series they concluded that there was no correlation with bottom temperature and the movement of the Polar Front. Therefore they rejected Deacons argument that the circulation of the bottom water controlled the southward rise of the warm Deep Water and hence the location of the Polar Front.

[30] From the hydrographic sections we can extend in time the analysis of Antarctic Bottom Water in the Ona Basin presented by *Rubython et al.* [2001]. Variability in the Antarctic Bottom Water extends uniformly across the Ona Basin from 58.5°S to 60.5°S (Figure 4a) that is between the Polar Front and the Southern ACC front. In Figure 4b we have plotted Figure 3a from *Rubython et al.* [2001] and added the bottom temperature anomaly determined from the closest CTD stations in time and space. For the three points of comparison the standard deviation (2-degrees of freedom) of the difference is 0.0048°C.

[31] We extend the time series of bottom temperature anomalies using the CTD data Figure 4c. The temporal resolution of this time series is poor compared with the bottom pressure recorder time series. However, the cold anomaly evident in 1994 is matched by a cold anomaly of similar amplitude in 1999: a five year cycle? Between November 1999 and November 2000 the Antarctic Bottom Water across the Ona Basin warmed by 0.14°C. On Figure 4c we note the position of the Polar Front taken from the latitude of rapidly increasing zonally integrated transport in Figure 2. There is a correspondence between the Polar Front position and Antarctic Bottom Water temperature anomaly. When the Polar Front position is northerly the Ona Basin is covered in much colder Antarctic Bottom Water and when the Polar Front is southerly the Antarctic Bottom Water in the Ona Basin is warmer, evidence that the southward rise of warm Deep Water and the Polar Front are connected. Sir George Deacon postulated that the circulation of the deep water was responsible for this relationship. We do not yet know if this is correct or if the Polar Front position determines the deep circulation; however, this result contradicts the analysis of ATSR SST data presented by *Rubython et al.* [2001].

4.3. Topographic Control

[32] It seems unlikely that local topographic steering leads to the bimodal distribution of the Polar Front transport. The surface jet of the Polar Front is sited over a bathymetric rise on the southern edge of the West Scotia Ridge. This rise is roughly the same width as the Polar Front jet, and is around 700 m higher than the bathymetry on either side. There does not seem to be any correspondence between the southerly or northerly positions of the Polar Front and this rise (Figure 3). On a larger scale it does seem that the Polar Front is found south of the West Scotia Ridge except in 1999 when the Polar Front and Subantarctic Front merge and this allows the main jet of the Polar Front to cross onto the West Scotia Ridge. Therefore at the length scale given by the separation of the Polar Front by the zonally integrated transport, meridional variations in bathymetry do not seem to control the position of the Polar Front.

5. Total Transport Estimates

[33] In 1996, 1997 and 2000 direct velocity measurements were made through the water column at each CTD station using an acoustic Doppler current profiler attached to the CTD frame. We use these velocity observations to calculate the net geostrophic transport through Drake Passage.

[34] The patterns of horizontal distribution and amplitude of the near-bottom reference velocities are remarkably similar in each year (Figure 5d). There is a persistent westward jet with velocities greater than 20 cms^{-1} over the continental shelf near 60°S. Between 60°S and the Polar Front (in the Ona Basin) the rich eddy field has a highly variable bottom velocity implying large barotropic circulations. These exceed ±20 cms^{-1} in 1996. The Polar Front has consistent eastward bottom velocities between 10 and 20 cms^{-1}. Over the rougher topography of the Shackleton Fracture Zone and the Yagan Basin the near-bottom velocities have less variability and increase northward by about 10 to 15 cms^{-1} between 57°S and 55°S.

[35] We added the near-bottom reference velocities to the geostrophic velocities relative to zero at the DCL and integrated the transport south to north (Figures 5a, 5b, and 5c).

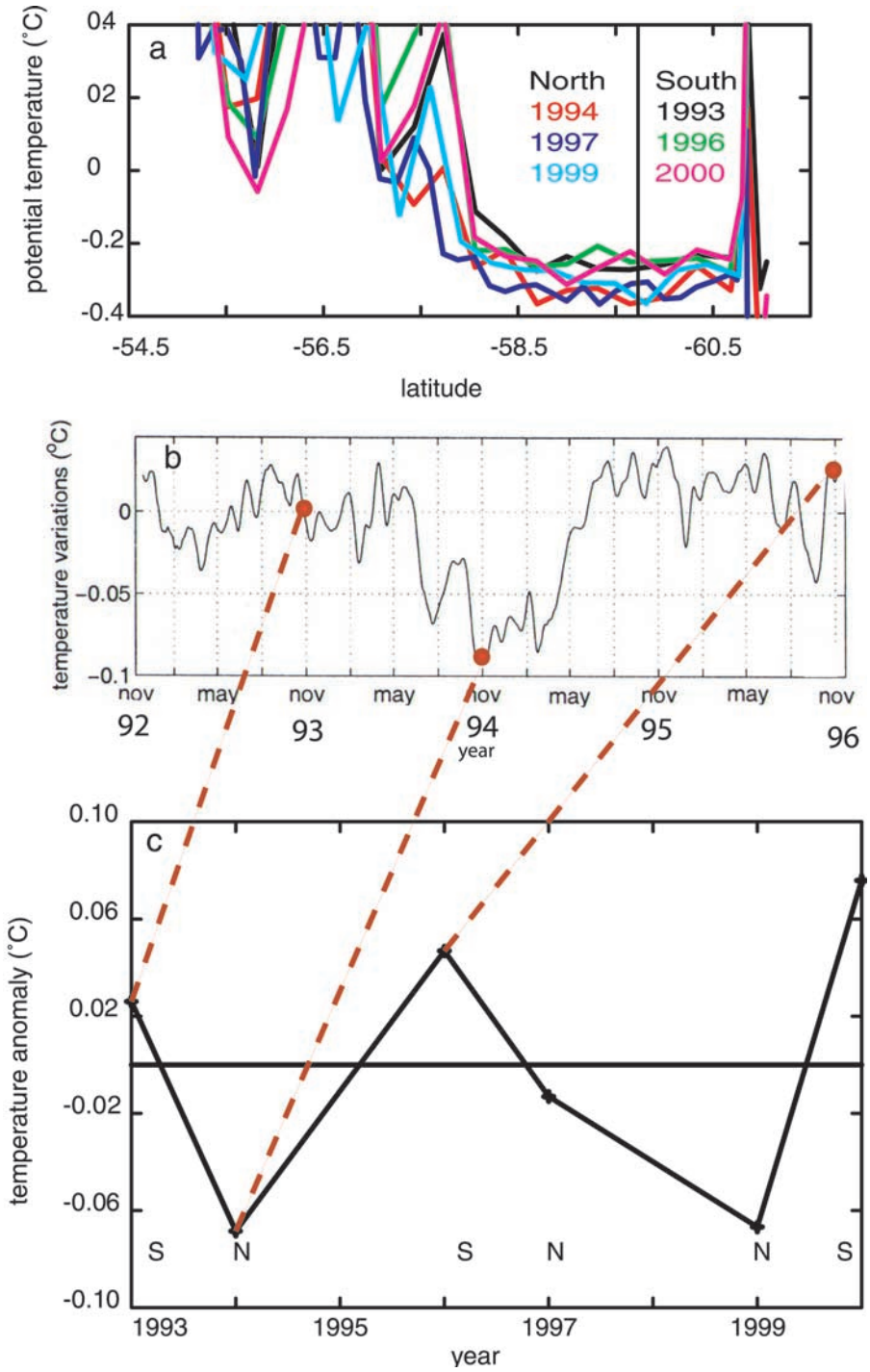

Figure 4. (a) Depth-averaged potential temperature within 50 m of bottom (Antarctic Bottom Water covers the Ona Basin between −58.5°S and −60.5°S) for the six SR1b sections. 1993 black, 1994 red, 1996 green, 1997 dark blue, 1999 light blue and 2000 mauve. The solid vertical line at 59°43.7S, 55°29.5W indicates the position of the bottom pressure recorder (BPR) discussed in the text. (b) Solid line is temperature anomalies (relative to the average temperature 1992 to 1996) from the BPR [*Rubython et al.*, 2001]. Red dots are the depth-averaged (50 m from bottom) temperature anomalies from the SR1b CTD station closest to the BPR at time corresponding to the section occupations. The standard deviation of the difference between the BPR and CTD anomalies is 0.0048°C. (c) Time series of bottom temperature anomalies from SR1b CTD stations closest to the BPR. The position of the Polar Front (north/south from the section-integrated baroclinic transport in Figure 2) is noted by the letters N or S.

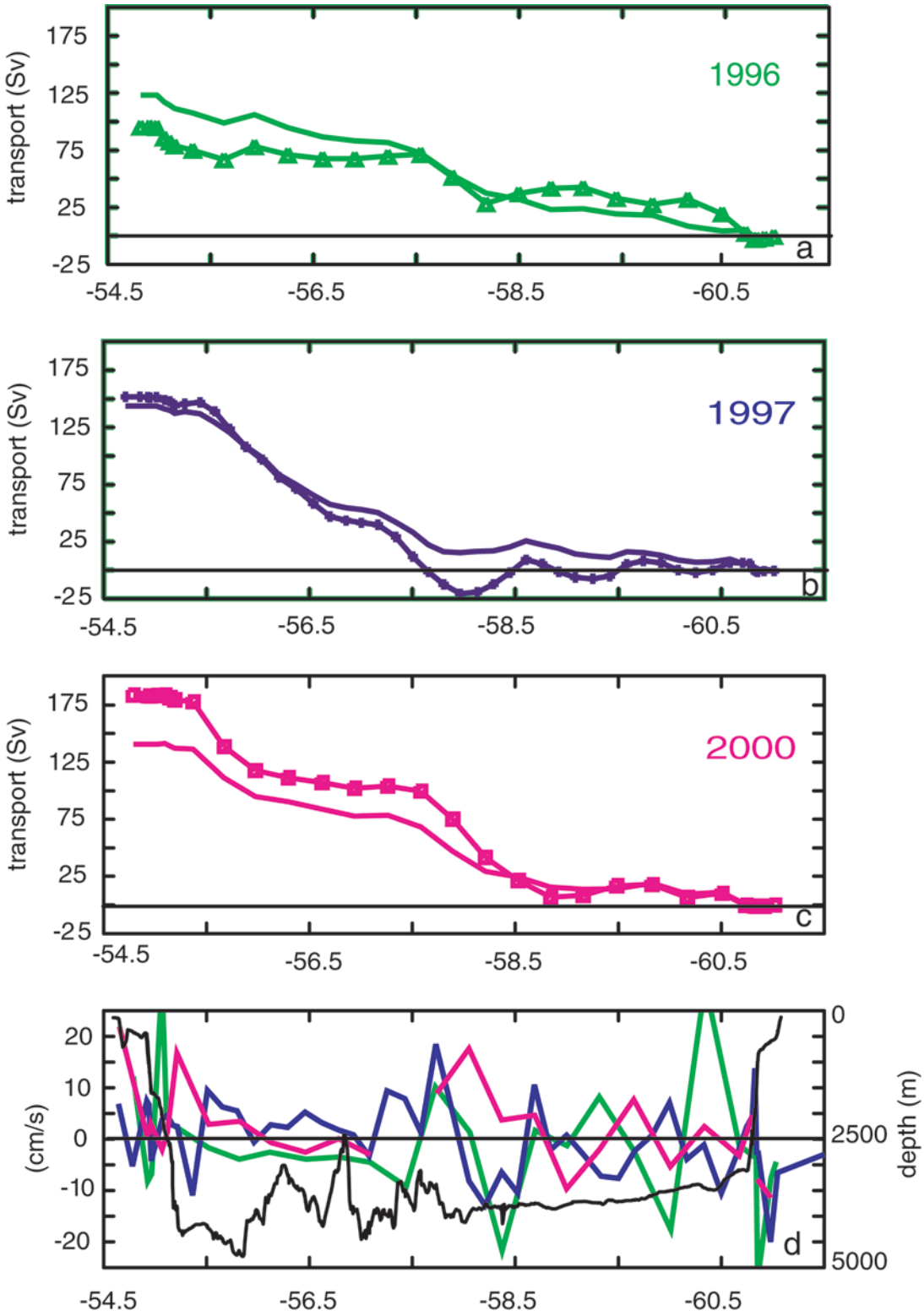

Figure 5. (a) Year 1996 geostrophic section-integrated transport in Sv relative to zero at the DCL (solid line) and integrated transport relative to near-bottom reference velocities derived from bottom track lowered acoustic Doppler current profiler measurements (symbols). (b) Year 1997. (c) Year 2000. (d) Near-bottom reference velocities used in Figures 5a–5c (1996 green, 1997 dark blue, and 2000 mauve). The bathymetry along the section is shown in black.

Table 3. Section-Integrated Geostrophic Transport Relative to the DCL (BC) and Relative to the LADCP Bottom-Track Reference Velocities (BT)[a]

Year	BC, Sv	BT, Sv	BT-BC, Sv	$\bar{v}$, cms^{-1}
1996	123	95	−28	−1.2
1997	144	152	8	0.3
2000	141	184	43	1.8
Mean	136	144	8	
SD, n-1	11.4	45	35.5	
Range	21	89		

[a]BT-BC is the transport due to the bottom reference velocities. $\bar{v}$ is the average reference velocity, calculated by dividing (BT-BC) by 24 Sv/cms^{-1}.

In two years the net transport increases due to the reference velocities and in one year decreases (Table 3).

[36] Previously we estimated that the error associated with the near-bottom velocity on each station to be about 0.2 cms^{-1}. A typical near bottom profile consists of 20 such estimates, but we will estimate the standard error of the mean near bottom velocity to be about $0.2/\sqrt{10} = 0.06$ cm/s. If this error accumulates randomly over 31 stations then the net error is 0.3 cms^{-1} or 8 Sv. Note at this stage that this error analysis assumes independent random errors and does not allow for unknown bias. It is a lower bond on the uncertainty.

[37] *Bryden and Pillsbury* [1977] analyzed flow through Drake Passage from six yearlong current meter records at 2700 m depth. They found that for the mean flow the average length of time required for independent through channel velocity measurements was 6.8 days. The timescale of the dominant velocity fluctuations of the mean flow is 15 days. The SR1b section takes five days to occupy so that the LADCP derived near-bottom velocities are characteristic of a snapshot rather than of the time-mean flow.

[38] *Bryden and Pillsbury* [1977] found that at 2700 m the mean flow varied between 7.6 to −2.9 cms^{-1} with a RMS amplitude of 2 cms^{-1} about its time-averaged value. The mean flow was 1.56 ± 1.44 cms^{-1} (= 39 ± 36 Sv). The LADCP derived near-bottom reference velocities (and transports) Table 3 lie comfortably within the mean estimated by *Bryden and Pillsbury* [1977].

5.1. Transport in Neutral Density Layers

[39] The geostrophic transports relative to the DCL in neutral density layers (Figure 6a and Table 4a) are similar year to year, particularly for the denser layers of circumpolar deep water where most of the transport occurs. The variability in layers lighter than γ_n = 27.0 kg/m^3 is large compared with the mean in that layer. The variation is driven by changes in density due to seasonal warming of the near-surface layers north of the Polar Front (i.e., changes in abundance of the water mass) rather than changes in the velocity field. The 1997 and 1999 sections were occupied later in the season.

[40] Although the layer transport anomalies (Figure 6b and Table 4b) are noisy the lowest transport year 1996 (123 Sv) has reduced transport over the whole density range. In the other years density classes have positive and negative anomalies including the highest transport year 1997 (144 Sv).

[41] The change in flux in neutral density layers due to the LADCP near-bottom reference velocities is given in Figure 7 and Table 5. In 1996 the reference velocities give a westward flux in all but the lightest and densest layers, resulting in a total flux of −27 Sv (westward). In 1997 and 2000 the reference velocities contribute a net eastward flux of 8 and 43 Sv respectively. The vertical distribution of this flux is different in these two years (Figure 7). In 2000 the extra flux accumulates mainly in the Lower Circumpolar Deep Water layers, while in 1997 the extra flux is distributed evenly across Subantarctic Mode Water, Antarctic Intermediate Water and Circumpolar Deep Water.

[42] Unexpectedly the near-bottom reference velocities contribute fluxes of the opposite sign to the Circumpolar Deep Water and Antarctic Bottom Water: when the eastward flux of Circumpolar Deep Water is enhanced the Antarctic Bottom Water flux is westward and vice versa. While this does not prove Deacon's hypothesis that the circulation of the densest layers controls the position of the southward rise of the Circumpolar Deep Water and the position of the Polar Front it does suggest an intimate link between the two.

5.2. Temperature Transport

[43] Although a comprehensive study of property transports is beyond the scope of this paper, some simple calculations are useful for comparison with previous authors. Transport or divergence of heat is a useful concept only where there is a net balance of volume. However, the volume transport-weighted mean temperature across a boundary can be used to give an indication of the way a property is changing in some region.

[44] *Georgi and Toole* [1982] report the volume transport-weighted mean temperature for their analysis of two Drake Passage sections. This quantity is the total property transport divided by the total volume transport, and in the Georgi and Toole analysis has the value 2.52°C. Georgi and Toole use the difference between this value and the equivalent value south of Africa (1.82 °C) to infer the heat lost by this sector of the ACC: essentially 0.7°C times 127 Sv.

[45] The transport-weighted mean temperatures in °C for our six sections are, respectively: 2.18, 2.10, 2.12, 2.28, 2.50, 2.18. Note that the range is 0.40°C. The two high values are for the fourth and fifth cruises, conducted in January 1998 and February 2000. In other words, the seasonal cycle, through heating of the surface layer where the velocities are greatest, introduces changes in the heat transported through Drake Passage with a range of 0.4 × 137 Sv°C, or 0.22 PW. A study of heat gained or lost along the track of the ACC using mean temperatures at the choke points must therefore make very careful consideration of the season signals in all the data used. We note that our February value of 2.50°C is not significantly different from that reported by Georgi and Toole for the 1975 Melville data.

6. Net Transport Through Drake Passage Measured During the International Southern Ocean Studies Program

[46] Two decades have elapsed since the International Southern Ocean Studies (ISOS) programme to measure the yearlong transport through Drake Passage. From those observations the annual average net transport of the Antarctic Circumpolar Current through Drake Passage was 124.7 ± 9.9 Sv above 2500 m [*Whitworth and Peterson*, 1985]

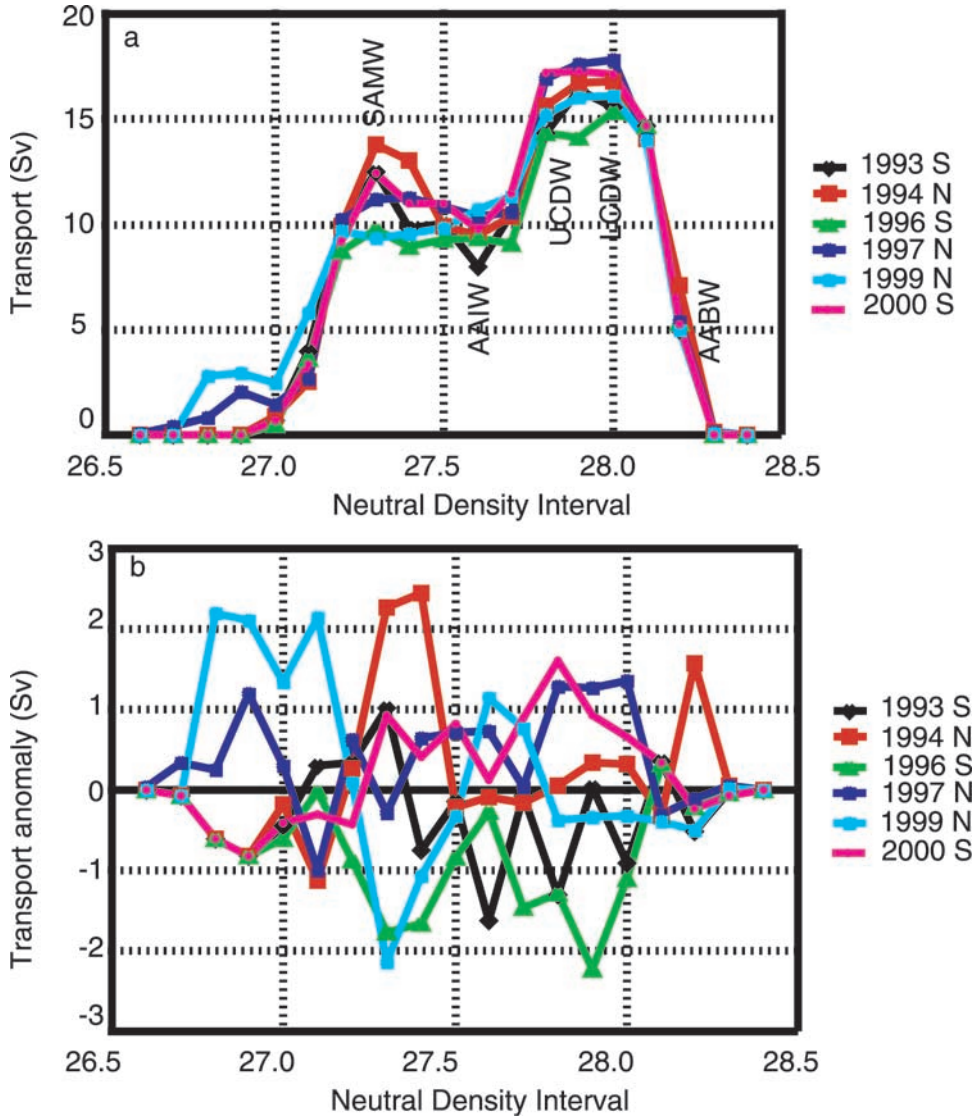

Figure 6. (a) Section-integrated geostrophic transport relative to the DCL in neutral density layers γ_N (layer width 0.1 kg/m^3) for the six SR1b hydrographic sections. The position of the Polar Front (north/south from the section-integrated baroclinic transport in Figure 2) is noted by the letters N or S. Some water masses are also indicated: Subantarctic Mode Water (SAMW), Antarctic Intermediate Water (AAIW), Upper and Lower Circumpolar Deep Water (U/L CDW), and Antarctic Bottom Water (AABW). (b) Transport anomalies relative to the 1993 to 2000 average transport in each layer. The density ranges of water masses are given in Table 4a.

(9.9 Sv is the standard deviation of the yearlong average and is not an error estimate of the average) and 9.1 ± 5.3 Sv below 2500 m [*Whitworth*, 1983], giving a total of 133.8 ± 11.2 Sv from January 1979 to February 1980. (We estimate the variability in this total transport as $\sqrt{9.9^2 + 5.3^2} = 11.2$ *Sv*.) This estimate of the average net transport through Drake Passage is one of the key numbers in the oceanographers cannon [*Rintoul and Sokolov*, 2000]; however, there is a large uncertainty in the mean; a point not widely appreciated, though stressed in the original calculations. Because the average transport of the ACC is a key number in the global ocean circulation and because the calculations using the ISOS data are spread over a number of papers it is valuable to review these in detail and to bring together a short summary.

[47] The ISOS mooring array consisted of 17 moorings deployed along a line between Cape Horn and Livingston Island (Figure 8). This section is 723 km long and moorings were deployed at separations of ~45 km in the northern and central Drake Passage and ~75 km in southern Drake Passage. *Sciremammano et al.* [1978], estimate (using the zero-crossing of the cross-correlation function between current meters) that the cross-passage scale of the through passage velocity fluctuations is on the order of 40 km so that velocity measurements at adjacent moorings are independent. The mooring array was deployed in January 1979 and recovered in February 1980. Pressure gauges were placed on the 500 m and 2500 m contours at either side of the passage. Three full depth CTD sections were occupied during the year of the mooring array: in January 1979;

Table 4a. Geostrophic Transport (Sv) Relative to the DCL in Neutral Density Layers[a]

Layer	γ_N, kgm^{-3}		1993	1994	1996	1997	1999	2000	Average
1	26.6	26.7	0.0	0.0	0.0	0.0	0.0	0.0	0.0
2	26.7	26.8	0.0	0.0	0.0	0.4	0.0	0.0	0.1
3	26.8	26.9	0.0	0.0	0.0	0.8	2.8	0.0	0.6
4	26.9	27.0	0.0	0.0	0.0	2.0	2.9	0.0	0.8
5	27.0	27.1	0.6	0.9	0.5	1.4	2.4	0.7	1.1
6	27.1	27.2	4.0	2.5	3.6	2.7	5.8	3.4	3.7
7	27.2	27.3	10.0	9.9	8.7	10.3	9.7	9.2	9.6
8	27.3	27.4	12.5	13.8	9.7	11.2	9.4	12.4	11.5
9	27.4	27.5	9.9	13.1	9.0	11.2	9.5	11.0	10.6
10	27.5	27.6	10.0	9.9	9.3	10.9	9.8	11.0	10.1
11	27.6	27.7	8.0	9.5	9.4	10.3	10.8	9.7	9.6
12	27.7	27.8	10.5	10.4	9.1	10.6	11.3	11.5	10.6
13	27.8	27.9	14.3	15.7	14.3	16.9	15.2	17.2	15.6
14	27.9	28.0	16.4	16.7	14.1	17.6	16.0	17.3	16.4
15	28.0	28.1	15.5	16.8	15.4	17.8	16.1	17.1	16.5
16	28.1	28.2	14.7	14.0	14.7	14.0	14.0	14.7	14.4
17	28.2	28.3	5.0	7.1	5.3	5.4	5.0	5.3	5.5
18	28.3	28.4	0.0	0.1	0.0	0.1	0.1	0.0	0.1
19	28.4	28.5	0.0	0.0	0.0	0.0	0.0	0.0	0.0
			131.4	140.4	123.1	143.8	140.9	140.4	136.7

[a]Water masses within the ACC are defined by extrema of various property distributions but can be roughly separated by the following neutral density layers (kg/m^3) (following *Speer et al.* [2000]): SAMW and AAIW 27.0–27.5; UCDW 27.5–28; LCDW or NADW 28–28.2; and AABW denser than 28.2. The sum of layer transports is given in the final row.

April 1979; and January 1980. CTD stations were taken mid-way between moorings so that a pair of hydrographic stations spans each current meter mooring.

[48] The total transport through Drake Passage is constructed from the sum of four separate components (Figure 9):

[49] 1. Total geostrophic transport between 2500 m and 500 m from hydrographic transport moorings at the northern and southern boundaries of Drake Passage referenced to the direct velocity estimates at 500 m from the current meter array.

[50] 2. Total geostrophic transport between 500 m and the surface from historical hydrographic observations referenced to the direct velocity estimates at 500 m.

Table 4b. Transport Anomalies Relative to the 1993–2000 Mean Transport[a]

Layer	γ_N, kgm^{-3}		1993	1994	1996	1997	1999	2000
1	26.6	26.7	0.0	0.0	0.0	0.0	0.0	0.0
2	26.7	26.8	−0.1	−0.1	−0.1	0.3	−0.1	−0.1
3	26.8	26.9	−0.6	−0.6	−0.6	0.2	2.2	−0.6
4	26.9	27.0	−0.8	−0.8	−0.8	1.2	2.1	−0.8
5	27.0	27.1	−0.5	−0.2	−0.6	0.3	1.3	−0.4
6	27.1	27.2	0.3	−1.1	0.0	−1.0	2.1	−0.3
7	27.2	27.3	0.3	0.3	−0.9	0.6	0.1	−0.4
8	27.3	27.4	1.0	2.3	−1.8	−0.3	−2.1	0.9
9	27.4	27.5	−0.8	2.4	−1.7	0.6	−1.1	0.4
10	27.5	27.6	−0.1	−0.2	−0.8	0.7	−0.3	0.8
11	27.6	27.7	−1.6	−0.1	−0.3	0.7	1.1	0.1
12	27.7	27.8	−0.1	−0.2	−1.5	0.0	0.8	0.9
13	27.8	27.9	−1.3	0.1	−1.3	1.3	−0.4	1.6
14	27.9	28.0	0.0	0.3	−2.2	1.3	−0.3	0.9
15	28.0	28.1	−0.9	0.3	−1.1	1.4	−0.3	0.7
16	28.1	28.2	0.4	−0.3	0.3	−0.3	−0.4	0.3
17	28.2	28.3	−0.5	1.6	−0.2	−0.1	−0.5	−0.2
18	28.3	28.4	0.0	0.1	0.0	0.1	0.0	−0.1
19	28.4	28.5	0.0	0.0	0.0	0.0	0.0	0.0
			−5.3	3.7	−13.5	7.1	4.2	3.7

[a]The sum of layer transports is given in the final row.

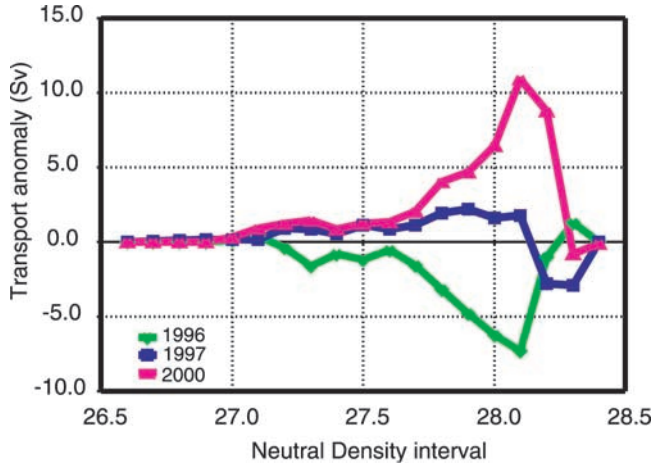

Figure 7. Section-integrated geostrophic transport due to the near-bottom reference velocities (derived from bottom track lowered acoustic Doppler current profiler measurements) in neutral density layers γ_N (layer width 0.1 kg/m^3).

[51] 3. Estimates of the transport deeper than 2500 m from hydrography and current meters.

[52] 4. Transport at the continental boundaries between 2500 and 500 m from current meters. The critical analysis is determining the average 500 m cross-passage velocity by combining the direct current meter measurements and the three hydrographic sections. By levelling the pressure gauges relative to the three 500 m average velocity estimates, a continuous time series of the absolute velocity at 500 m is obtained. The calculation of these four components and their error estimates is described below.

[53] Two moorings at either side of the passage (NT and ST, Figure 8) were instrumented with temperature/pressure gauges between 2500 m and 500 m [*Whitworth*, 1983]. Average historical θ/S relationships were used to estimate salinity to calculate dynamic heights from which the relative

Table 5. Total Transport in Neutral Density Layers for 1996, 1997, and 2000 Relative to Near-Bottom LADCP Velocities[a]

Layer	γ_N, kgm^{-3}	γ_N	1996, Sv	Anom, Sv	1997, Sv	Anom, Sv	2000, Sv	Anom, Sv
1	26.6	26.7	0.0	0.0	0.0	0.0	0.0	0.0
2	26.7	26.8	0.0	0.0	0.5	0.1	0.0	0.0
3	26.8	26.9	0.0	0.0	1.0	0.1	0.0	0.0
4	26.9	27.0	0.0	0.0	2.2	0.2	0.0	0.0
5	27.0	27.1	0.6	0.1	1.5	0.1	1.0	0.3
6	27.1	27.2	4.0	0.4	2.9	0.2	4.3	0.9
7	27.2	27.3	8.3	−0.4	11.2	0.9	10.5	1.3
8	27.3	27.4	8.1	−1.6	12.1	0.9	13.9	1.4
9	27.4	27.5	8.1	−0.8	11.8	0.6	11.9	0.9
10	27.5	27.6	8.1	−1.2	12.0	1.1	12.2	1.3
11	27.6	27.7	8.8	−0.5	11.2	0.9	11.1	1.4
12	27.7	27.8	7.5	−1.6	11.7	1.1	13.5	2.1
13	27.8	27.9	11.2	−3.2	18.8	1.9	21.3	4.0
14	27.9	28.0	9.4	−4.8	19.9	2.2	22.0	4.7
15	28.0	28.1	9.1	−6.2	19.4	1.6	23.6	6.4
16	28.1	28.2	7.4	−7.3	15.8	1.8	25.6	10.9
17	28.2	28.3	4.3	−1.0	2.6	−2.8	14.0	8.8
18	28.3	28.4	1.3	1.3	−2.8	−2.9	−0.8	−0.8
19	28.4	28.5	0.0	0.0	0.0	0.0	−0.1	−0.1
			96.3	−26.8	151.8	8.0	183.9	43.5

[a]Anom is the transport due to the reference velocities. The sum of the layer transports and anomalies are given in the final row.

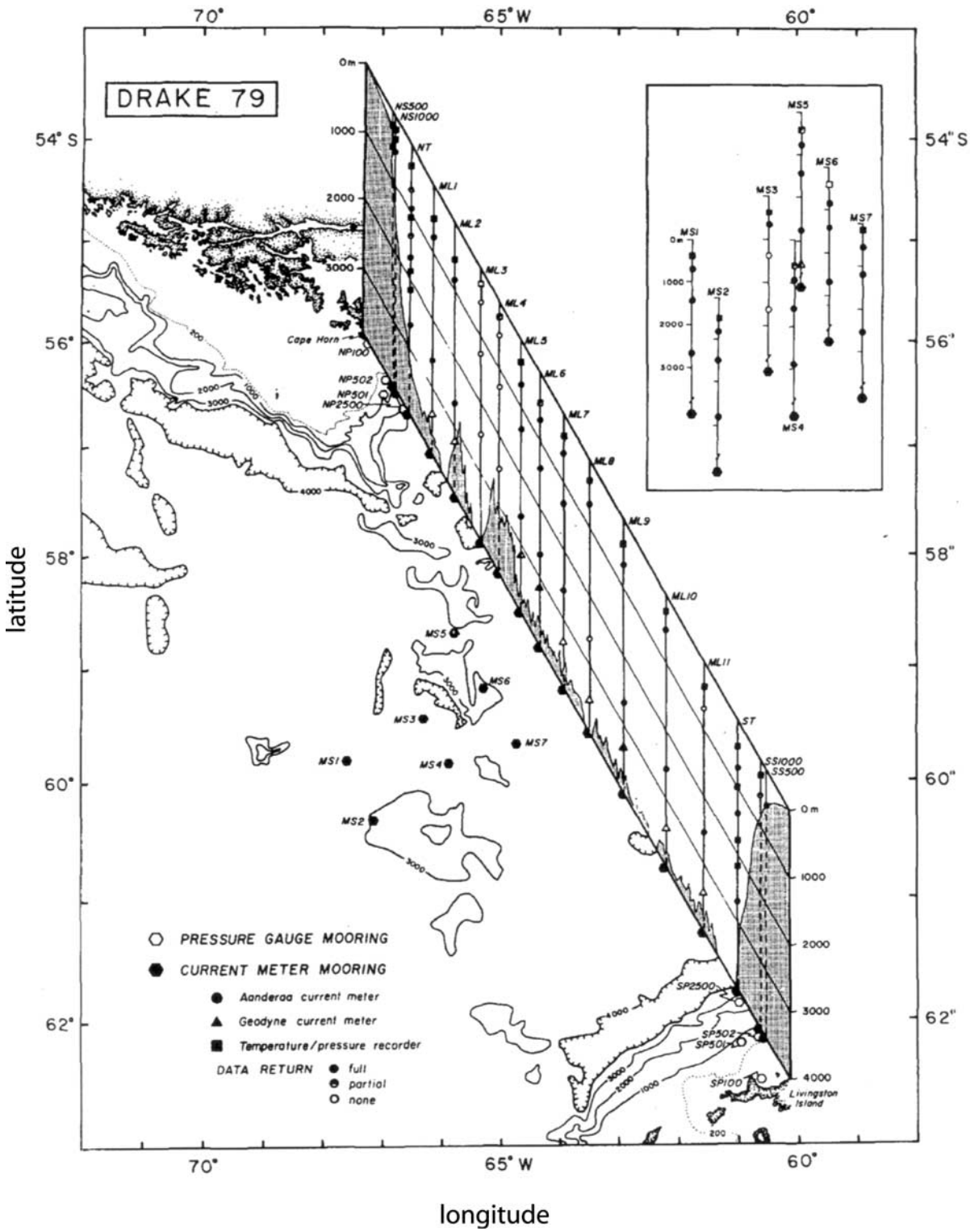

Figure 8. The DRAKE 79 moored array indicating instrument locations and data return. From *Whitworth et al.* [1982, Figure 1], reprinted by permission.

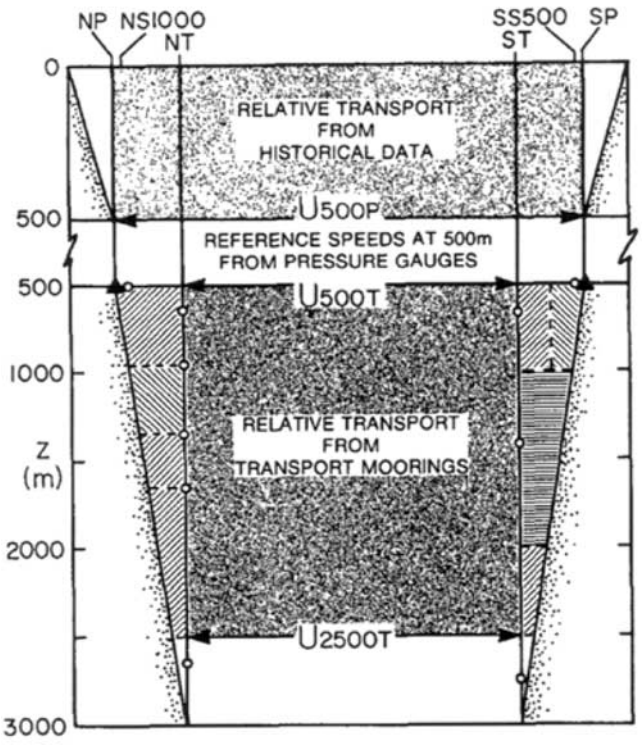

Figure 9. Schematic cross section of Drake Passage illustrating the procedure used by *Whitworth* [1983] to calculate the net transport (shaded area). Transport in the north and south slope regions (hatched areas) is estimated using direct measurements from current meters (open circles). From *Whitworth and Peterson* [1985, Figure 1], reprinted by permission.

geostrophic transport between 2500 m and 500 m was determined.

[54] The use of average θ/S relationships could introduce error due to θ/S variability. We examined 12 stations at each side of the Passage from each of our six cruises. The standard deviation of salinity at theta levels would be equivalent to 0.03 and 0.06 dynm respectively at the north and south side of the Passage if the salinity deviation occurred as an anomaly through the entire water column. This represents a worst case. We might therefore estimate that the uncertainty in north-south dynamic height difference from this source is no more than 0.07 dynm (about 7 Sv) and almost certainly rather less.

[55] While using only average θ/S relationships, *Whitworth* [1983] did consider uncertainty due to the presence of anomalous temperatures in the water column, and concluded that from that source the largest errors in dynamic height when atypical colder or warmer waters are present was 10% (~8 Sv). The mean dynamic height (relative to 2500 m at the northern mooring is 1.37 ± 0.05 dynm, and at the southern mooring is 0.58 ± 0.02 dynm giving a mean cross passage dynamic height difference of 0.79 dynm (about 77 Sv).

[56] The relative transport between 500 m and the surface was calculated from historical hydrographic data [*Whitworth*, 1983]. Observations from 20 cruises (only four of which were made in winter) were used to calculate the transport of the upper 500 m relative to 500 m. The average transport was 6.4 ± 0.7 Sv with a range of 2.2 Sv.

[57] Using the current meter data on the NT and ST moorings, velocities were extrapolated to the continental slope regions [*Whitworth and Peterson*, 1985]. The average transport in the slope regions is only 2 Sv but on occasions the instantaneous transport exceeds 15 Sv as meandering fronts that moved out of the mooring array were then included in the total transport estimates. This extrapolated transport reduced the variability of the total transport.

[58] The pressure gauges at 500 m provide reference speeds for the relative geostrophic transport in the upper 500 m and between 2500 m and 500 m as now described. Assume that the large-scale flow is in geostrophic balance, then the horizontal pressure gradient is balanced by the Coriolis force,

$$u = -\frac{1}{f_0 \rho_0} \frac{\partial p}{\partial y}. \tag{1}$$

Pressure gauges cannot give this balance directly as the pressure gradient must be evaluated along geopotential surfaces and the depths of the geopotential surfaces are unknown. For two pressure gauges nominally positioned at depth z_1 (Figure 10), the measured pressure gradient will differ from the pressure gradient on a geopotential by a constant. This constant is proportional to the difference in depth of the pressure gauges from a line of constant geopotential, is independent of time and can be evaluated if the average geostrophic speed between the pressure gauges is known at one time.

[59] We have

$$u = -\frac{1}{f_0 \rho_0} \frac{p_2|_g - p_1|_g}{\Delta y}, \tag{2}$$

where the subscript g indicates evaluation along a geopotential. For one pressure gauge not on the geopotential we can adjust the pressure by assuming that the ocean is in hydrostatic equilibrium

$$\frac{\partial p}{\partial z} = -\rho g, \tag{3}$$

and integrating between z_1 and the geopotential at z_2, such that the pressure difference is

$$\int_{P1|_{z1}}^{P2|_{z2}} dp = -\rho_0 g \int_{z_1}^{z_2} dz. \tag{4}$$

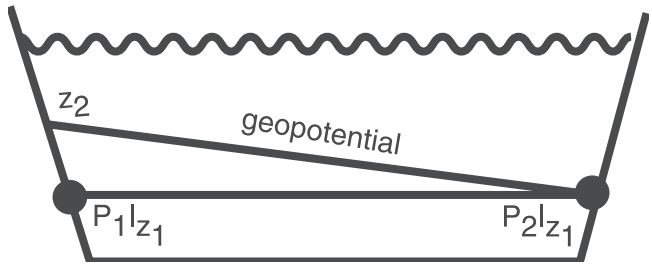

Figure 10. Illustration showing the relationship of pressure gauges nominally positioned at depth z_1 to a geopotential surface that passes through pressure gauge P_2 but is found at shallower depths above pressure gauge P_1.

Table 6. Average Total Transport Between 2500 m and the Surface Referencing The Baroclinic Shear From the Hydrographic Cruises to the Current Meters[a]

Date	Average Total Transport, Sv	Error, Sv
January 1979	117	15
April 1979	144	6
January 1980	137	10

[a]The error estimate is the standard deviation of the offsets from the current meters converted into a transport error. Note that 1 cms^{-1} error gives a transport error of 17.5 Sv above 2500 m.

Therefore the pressure at z_1 is related to the pressure at the geopotential by

$$p_1\big|_g = p_1\big|_{z1} - \rho_0 g \int_{z_1}^{z_2} dz. \tag{5}$$

Substituting (5) into (2) and rearranging (note that $p_2|_g \equiv p_2|_{z1}$).

$$u = \frac{1}{\rho_0 f_0}\left(\frac{p_2|_{z1} - p_1|_{z1}}{\Delta y}\right) + \frac{g}{f_0 \Delta y}\int_{z_1}^{z_2} dz \tag{6}$$

The second term on the right hand side of (6) is a constant proportional to the difference in depth of pressure gauge one from the geopotential. The constant is independent of time and can be evaluated from (6) if the average geostrophic speed u between the two pressure gauges can be determined at some time. Evaluation of this constant is referred to as levelling the pressure gauges.

[60] The average through passage speed was determined by referencing the geostrophic velocities relative to zero at 2500 m from hydrography to the current meter velocities. Each current meter provided an estimate of the geostrophic reference velocity. For moorings with more than one current meter the geostrophic reference velocities were averaged. Where current meter moorings were lost, linear interpolation was used to provide reference velocities across the gap. There are three estimates for the absolute cross passage speed, one for each hydrographic section.

[61] Errors in net transport were calculated as the standard deviation of the transport estimates at 9 out of 15 moorings with more than one current meter applied to the remaining six moorings. The error estimate for the entire section is then the square root of the sum of the 15 transport variances at each mooring. The mean transports and their errors are given in Table 6. The pressure gauge offset for the three estimates of the average 500 m speed are given in Table 7.

[62] The range and standard deviation of the pressure gauge offsets 1.52 cms^{-1} and 0.83 cms^{-1} respectively gives the probable transport error arising from the levelling of the pressure gauges as 25 Sv (range) and 14 Sv (standard deviation). Once the pressure gauges have been levelled they are used to provide a yearlong time series of the average cross passage speed at 500 m, and consequently the net transport time series.

Table 7. Area Weighted Average Speed at 500 m and the Pressure Gauge Leveling Constant Given in Equation (6)

Date	Average 500 m Speed, cms^{-1}	$\frac{g}{f_0\Delta y}\int_{z_1}^{z_2} dz$, cms^{-1}
January 1979	10.85	53.14
April 1979	10.25	52.94
January 1980	11.29	54.46

Table 8. Total Transport Error Arising in the Different Components of The Total Transport Estimates Taken Directly From the Whitworth Papers[a]

Error Source	Error Range, Sv
Relative transport due to dynamic heights (2500 m to 500 m)	5–10
Pressure gauge leveling	14–25
Relative transport range from mean historical dynamic heights (500 m to surface)	2
Transport below 2500 m	5.3

[a]Whitworth papers include *Whitworth* [1983], *Whitworth and Peterson* [1985], and *Whitworth et al.* [1982].

[63] Whitworth and coauthors were keenly aware of how critical the step of levelling the pressure gauges was and their reliance on estimates of the average cross passage speed at 500 m. This point was emphasised by *Whitworth et al.* [1982, p. 813], "These gaps, especially the northern one which is near the location of the Subantarctic Front (between ML2 and ML5, Figure 8), seriously reduce the accuracy of any attempt to characterize the flow at 500 m from direct current measurements."

[64] The reference velocity at 500 m between ML2 and ML5 (separated by 125 km) was estimated by linear interpolation. Unfortunately the missing moorings were located at critical positions close to and between the historical positions of the Subantarctic Front and Polar Front. *Whitworth and Peterson* [1985] wrote "When a front (either the Subantarctic Front or Polar Front) is in the gap between ML2 and ML5, the spatially averaged current will be underestimated... and when ... a front is near ML2 or ML5 the direct measurements are likely overestimated." Estimates for the potential magnitude of this error were not given but could be expected to be large for strong barotropic, spatially inhomogeneous flow.

[65] The transport below 2500 m was estimated [*Whitworth*, 1983] using the net speed at 2500 m and six ISOS hydrographic sections that sampled close to the bottom. The average baroclinic transport below and relative to 0 cms^{-1} at 2500 m was −6.7 Sv (i.e., westward). The average speed at 2500 m was 2.09 ± 0.69 cms^{-1} giving a transport of 15.8 ± 5.3 Sv. Therefore the average transport below 2500 m was 9.1 ± 5.3 Sv.

[66] The error estimates in the different components of the total transport (Table 8) are estimated as root, sum, squares and give errors of 15 to 27 Sv. Therefore the total transport is 134 Sv ± 15 to 27 Sv with a standard deviation of the yearlong transport of 11.2 Sv.

7. Barotropic Versus Baroclinic Variability

[67] A widely held tenet is that the variability of Drake Passage transport is mainly barotropic and can be monitored using the across passage pressure difference. This idea first arose in the work by *Whitworth and Peterson* [1985] who were able to compare yearlong time series of total transport and across passage pressure difference. First, they noted that the net transport and across passage pressure difference time series are in phase and coherent at virtually all frequencies.

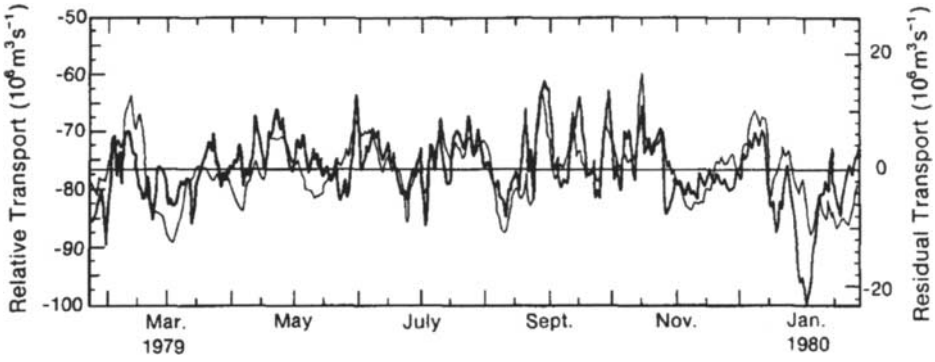

Figure 11. From *Whitworth and Peterson* [1985, Figure 6]. Thick line geostrophic transport between 500 and 2500 m relative to 500 m; the thin line is the transport residuals ($T - T'$) where $T' = 18.7 - 81U_{500P}$ is predicted transport, U_{500P} is the velocity time series derived from the pressure gauges at 500 m, and T is a 40 hour low-passed time series of total transport. The model residuals are equal to the baroclinic variability in the upper ocean that is neglected by fitting total transport to cross passage pressure difference.

Second, that the range in the across passage average speed at 500 m if barotropic, would give a transport range of 59 Sv; the actual range in net transport was 54 Sv. They concluded that a large part of the transport variability "appears to be in the barotropic field, and pressure difference should provide a good estimate of transport."

[68] The baroclinic transport (January 1979 to February 1980) relative to and above 2500 m [*Whitworth*, 1983] has a mean transport of 87 ± 5.5 Sv (range 70 to 100 Sv) and the absolute transport above 2500 m for the same period is 124.7 ± 9.9 Sv (range 95 to 149 Sv) [*Whitworth and Peterson*, 1985]. Therefore although the barotropic transport variability contributes most to the net transport variability (9.9 Sv) the baroclinic transport variability (5.5 Sv) is a significant portion of the total variability. The baroclinic transport range also contributes 30 Sv to the net transport range of 54 Sv.

[69] From January 1979 to February 1980 the net transport and the across passage pressure difference at 500 m had a correlation coefficient of 0.8 and explained 65% of the variance in net transport [*Whitworth and Peterson*, 1985] and this relationship was used as a linear model between cross passage pressure difference and net transport. Using this model to predict transport, transport residuals (measured-modelled transport) had a standard deviation of 5.9 Sv and a range of 39 Sv. The baroclinic transport between 500 and 2500 m relative to 500 m had a mean transport of 77 ± 5.3 Sv and a range of 29 Sv and tellingly, was coherent with the model residuals (Figure 11). Hence estimates of the transport variability through Drake Passage based solely on cross pressure difference underestimate the actual variability as they do not account for any (significant) baroclinic variability. Therefore we conclude that the baroclinic variability is an important contribution to the total variability and that across passage pressure difference is not an accurate indicator of variability in net transport.

8. Summary and Conclusions

[70] From 1975 to 2000 the average baroclinic transport (relative to and above 3000 m) is 107.3 ± 10.4 Sv, and there is no difference in average transports calculated for earlier and later portions of the time series. Therefore over 25 years the baroclinic transport through Drake Passage has been steady.

[71] The average net baroclinic transport relative to the bottom is 136.7 ± 7.8 Sv for six hydrographic sections across Drake Passage between 1993 and 2000. This transport occurs at three fronts: (south to north) the Southern ACC front carrying 9.3 ± 2.4 Sv; the Polar Front carrying 57.5 ± 5.7 Sv and; the Subantarctic Front carrying 53 ± 10 Sv. Occasionally the Polar Front and Subantarctic Front merge to carry a total transport of order 110 Sv. Between the Southern ACC Front and Polar Front there is a rich eddy field with recirculations of order 10 Sv and the average net transport within the eddy field is around 16 Sv.

[72] The location of the Polar Front (indicated by a rapid increase in the section-integrated transport) is bimodal: in 1994, 1997 and 1999 the position is 90 km north of its position in 1993, 1996 and 2000. The position of the Polar Front (north/south) seems to be related to: (1) the average section-integrated baroclinic transport (high/low); (2) temperature anomaly of Antarctic Bottom Water (cold/warm); and (3) Antarctic Bottom Water flux (westward/eastward), evidence that Deacon's hypothesis that the Polar Front position is related to the circulation of dense bottom water.

[73] We calculate baroclinic transport relative to the DCL in neutral density layers. The largest transports are found in density classes of the Circumpolar Deep Water. Except for the lowest transport year (1996) which has reduced transport in all density classes no systematic pattern was identified relating changes in top-to-bottom transport to changes in particular density layers.

[74] Using accurate near-bottom velocities measured by an LADCP as reference velocities we calculated the total net transport in three years. These estimates range from 95 to 184 Sv), a range of 88 Sv. Even considering the large uncertainty (27 Sv) of the average net ISOS transport values, this range does not appear to be consistent with the range of net transports from the ISOS array of 95 to 149 Sv; a range of 54 Sv: the error budget due to the contributions of the LADCP data may be significantly worse than our estimate has allowed.

[75] Finally we reviewed a series of papers by Whitworth and co-authors that calculated the flux and variability through Drake Passage from the ISOS data. The average net transport from January 1979 to February 1980 was 134 Sv with a standard deviation of 11.2 Sv, but we highlighted that the uncertainty of the average lies between 15 and 27 Sv. We also re-examined the conclusion that transport variability was principally barotropic and that variability of the net transport could be monitored using pairs of pressure gauges spanning Drake Passage. From the ISOS results net transport variability above 2500 m is partitioned between the net and baroclinic components in the ratio (net/baroclinic) of 9.9/5.5 Sv.

[76] Hydrographic observations of the Antarctic Circumpolar Current in Drake Passage made during WOCE have improved our knowledge of the distribution and variability of the baroclinic structure: particularly the location, width and transport of the major fronts. However, the newer methods of direct velocity observations using ADCP's (shipboard and lowered) have not significantly added to our knowledge of the net transport or net variability of the Antarctic Circumpolar Current, and hence of our ability to understand the forcing that sets these. The ISOS data still stand out as the definitive observations in this regard.

[77] For the future we must expand the Drake Passage time series observations. To determine and monitor the total transport requires measurements of the baroclinic and barotropic components of the flow. Profiling CTD/current meters on either side of Drake Passage would determine the baroclinic flow. A combination of absolute altimetric observations (once the gravity missions begin) and bottom pressure measurements will determine the absolute total geostrophic surface flow. Referencing the baroclinic observations to the average absolute surface speed will give the total transport.

[78] **Acknowledgments.** The observations presented in this paper have been obtained with help from many scientists from SOC, BAS and Universities around the UK. Such a unique time series cannot be maintained without these many unselfish contributions. The RRS *James Clark Ross* and her crew have ensured the success of each years' programme and they continue to welcome us aboard, despite our requirement to stop the ship for hydrographic observations in Drake Passage! This paper is a contribution to the core strategic research programme Ocean Variability and Climate of the James Rennell Division for Ocean Circulation and Climate at the Southampton Oceanography Centre.

References

Bacon, S., H. M. Snaith, and M. J. Yelland, An evaluation of some recent batches of IAPSO standard seawater, *J. Atmos. Oceanic Technol.*, *17*, 854–861, 2000.

Beal, L. M., and H. L. Bryden, The velocity and vorticity structure of the Agulhas Current at 32°S, *J. Geophys. Res.*, *104*, 5151–5176, 1999.

Bryden, H. L., and R. D. Pillsbury, Variability of deep flow in the Drake Passage from year-long current measurements, *J. Phys. Oceanogr.*, *7*, 803–810, 1977.

Deacon, G. E. R., The hydrology of the Southern Ocean, *Disc. Rep.*, *15*, 122 pp., 1937.

Egbert, G. D., and M. G. G. Bennett, TOPEX/POSEIDON tides estimated using a global inverse model, *J. Geophys. Res.*, *99*, 24,821–24,852, 1994.

Ganachaud, A., and C. Wunsch, Improved estimates of global ocean circulation, heat transport and mixing from hydrographic data, *Nature*, 453–456, 2000.

Georgi, D. T., and J. M. Toole, The Antarctic Circumpolar Current and the oceanic heat and freshwater budgets, *J. Meteorol. Res.*, *40*, suppl., 183–197, 1982.

King, B. A., E. Firing, and T. M. Joyce, Shipboard observations during WOCE, in *Ocean Circulation and Climate*, edited by R. Dmowska, J. R. Holton, and H. Rossby, Sect. 3, pp. 99–121, Academic, San Diego, Calif., 2001.

Locarnini, R. A., T. Withworth III, and W. D. Nowlin, The importance of the Scotial Sea on the outflow of Weddell Sea Deep Water, *J. Mar. Res.*, *51*, 135–153, 1993.

Orsi, A. H., T. Whitworth III, and W. D. Nowlin Jr., On the meridional extent and fronts of the Antarctic Circumpolar Current, *Deep Sea Res. Part I*, *42*(5), 641–673, 1995.

RD Instruments, Direct reading and self contained broadband acoustic Doppler current profiler, *P/N 951–6046–00*, RD Instruments, San Diego, Calif., 1995.

Rintoul, S. R., and S. Sokolov, Baroclinic transport variability of the Antarctic Circumpolar Current south of Australia (WOCE repeat section SR3), *J. Geophys. Res.*, *105*, 2815–2832, 2000.

Roether, W. R., R. Schilitzer, A. Putzka, P. Bening, and K. Bulsiewicz, A chlorofluromethane and hydrographic sectrion across Drake Passage: Deep water ventilation and meridional property transport, *J. Geophys. Res.*, *98*, 14,423–14,435, 1993.

Rubython, K. E., K. J. Heywood, and J. M. Vassie, Interannual variability of bottom temperatures in Drake Passage, *J. Geophys. Res.*, *106*(C2), 2001.

Sandwell, D. T., and W. H. F. Smith, Marine gravity anomalies from Geosat and ERS 1 satellite altimeters, *J. Geophys. Res.*, *102*, 10,039–10,054, 1997.

Sciremammano, F. J., R. D. Pillsbury, J. S. Bottero, R. E. Still, A compilation of observations from moored current meters, vol. XI, Currents, temperature and pressure in the Drake Passage during F Drake 76, *78-2*, Sch. of Oceanogr., Oregon State Univ., Corvallis, Ore., 1978.

Speer, K., S. R. Rintoul, and B. M. Sloyan, The diabatic Deacon Cell, *J. Phys. Oceanogr.*, *30*(12), 3212–3222, 2000.

Thompson, S. R., Sills of the global ocean: A compilation, *Ocean Model.*, *109*, 7–9, 1995.

Visbeck, M., Deep velocity profiling using lowered acoustic Doppler current profiler: Bottom track and inverse solutions, *J. Atmos. Oceanic Technol.*, *19*(5), 794–807, 2002.

Whitworth, T., III, Monitoring the transport of the Antarctic Circumpolar Current at Drake Passage, *J. Phys. Oceanogr.*, *13*(11), 2045–2057, 1983.

Whitworth, T., III, and R. G. Peterson, Volume transport of the Antarctic Circumpolar Current from bottom pressure meaurements, *J. Phys. Oceanogr.*, *15*(6), 810–816, 1985.

Whitworth, T., III, et al., The net transport of the Antarctic Circumpolar Current through Drake Passage, *J. Phys. Oceanogr.*, *12*(9), 960–971, 1982.

WHPO, Requirements for WOCE Hydrographic Program data reporting (Rev. 2), in *WOCE Operations Manual*, sect.3.1.2, pp. 67/91, World Ocean Circ. Exp. Hydrogr. Prog. Off., 1991.

S. G. Alderson, S. A. Cunningham, and B. A. King, Southampton Oceanography Centre, Southampton, SO14 3ZH, UK. (sga@soc.soton.ac.uk; scu@soc.soton.ac.uk; bak@soc.soton.ac.uk)

M. A. Brandon, Open University, Milton Keynes MK7 6AA, UK. (M.A.Brandon@open.ac.uk)